Tagged molecule induced nanoparticle aggregation: Raman reporter-labeled immuno-Au aggregate as immuno-sensor

Chunyuan Song (宋春元), Zhuyuan Wang (王著元), Ruohu Zhang (张若虎), Jing Yang (杨 晶), Xuebin Tan (谈学斌), and Yiping Cui (崔一平)*

Advanced Photonics Center, Southeast University, Nanjing 210096, China

**E-mail: cyp@seu.edu.cn*

Received July 14, 2009

A novel structure with high surface enhanced Raman scattering (SERS) activity and bio-specificity as a SERS-based immuno-sensor (named as Raman reporter-labeled immuno-Au aggregate) is demonstrated and employed for protein detection. In each fabrication process, the features of those aggregates are obtained and characterized by ultraviolet-visible (UV-Vis) extinction spectra, transmission electron microscopy (TEM) images, scanning electron microscopy (SEM) pictures, and SERS spectra. Experimental results indicate that proper amounts of the reporter molecules can result in the moderate aggregation morphologies of gold nanoparticles. Compared with the previously reported method using Raman reporter-labeled immuno-Au nanoparticles, more sensitive SERS-based protein detection is realized with this novel immuno-sensor.

OCIS codes: 160.4236, 290.5860, 300.6450.
doi: 10.3788/COL20100803.0309.

An immuno-sensor is a compact analytical device incorporating an antibody, an antigen or its fragment, either integrated within or intimately associated with a physiochemical transducer[1]. A large number of immunosensors based on the specific antibody-antigen interaction have been developed and provide a sensitive and selective tool for the estimation of proteins. Thereinto, surface enhanced Raman scattering (SERS) based immunoassay as a new immunoassay technique with higher sensitivity is known as a potent detection means for protein determination, which has been demonstrated to have the ability to detect picomole to femtomole concentrations[2]. Typically, this technique often makes use of the immune recognition of the specific binding between the undetermined proteins and the immuno-sensor named Raman reporter-labeled immuno-Au nanoparticles. The sample protein can be determined qualitatively or quantitatively by SERS signal produced by the reporter[3−8].

Though the distance dependent properties of gold nanoparticles have been explored to enhance the sensitivity of immuno-sensors[1], it has been well known that the respondence ability of SERS-based immunoassay depends strongly on the morphology (e.g., the size, shape, or aggregation) of the gold nanoparticles[9,10]. No Raman signal of reporter could be detected when small gold nanoparticles are used as a SERS substrate[11]. Krug *et al.* found that the isolated nanoparticle with average dimension at 25 nm was insufficient to enhance the Raman signals of the reporter absorbed on the surface of nanoparticle. Lamentedly, bigger gold nanoparticles can result in higher SERS activity, but their stability may decrease significantly with their size increasing when they are modified with Raman reporter[12,13]. Thus, many researchers have to carry out the SERS based-immunoassay using some small gold nanoparticles as immuno-sensor, and some additional activation treatments such as silver stain must be executed to obtain a high signal-to-noise ratio (SNR) of the SERS signal[14−20].

More recently, many researches make it clear that moderate aggregates of novel metal nanoparticles can generate a remarkable surface enhancement effect and provide feasibility to solve those problems mentioned above. It is well known that a surprising enhanced signal obtained at the junctions between nanoparticles of the aggregates is 2–40 times stronger than that obtained at an isolated nanoparticle[21−25]. Actually, the gold nanoparticle aggregates with a certain controlled size and high stability can be induced absolutely by adjusting the tagged molecules[26−28]. So, the reporter-labeled gold aggregates induced by tagged molecule with rich "hot spots" may have a stronger SERS activity without the sacrifice of high stability. It is assumed that with such novel immuno-sensor, the immunoassay can not only have no use for additional activation treatments of small nanoparticles, but also avoid the instability aroused by big nanoparticles. In this letter, a novel structure with high SERS activity and bio-specificity named Raman reporter-labeled immuno-Au aggregate is demonstrated and employed as an immuno-sensor for SERS-based protein detection successfully.

The reagents used in our experiment are given as follows. Hydrogen tetrachloroaurate(III) trihydrate ($HAuCl_4{\cdot}3H_2O$), 4-mercaptobenzoic acid (4MBA), and poly-L-lysine were purchased from Sigma. Trisodium citrate ($Na_3C_6H_5O_7{\cdot}2H_2O$) was obtained from Sinopharm Chemical Reagent Co., Ltd. Human antigen IgG, goat anti-human IgG antibody, rat antigen IgG, and bovine serum albumin (BSA) were purchased from Nanjing KeyGEN Biotechnology Co., Ltd. Deionized water (18 MΩ/cm) was used throughout the whole course of this experiment. The following buffer solutions were used: borate buffer solution (BBS, 2 mmol/L, pH = 9), tris buffer solution (TBS, 10-mmol/L tris, 150-mmol/L NaCl, pH = 7–8), and TBS/0.1% tween buffer

(10-mmol/L tris, 150-mmol/L NaCl, 0.1% tween 20, pH = 7–8).

100 mL of 10^{-4} g/mL $HAuCl_4$ was injected into a clean flask. After boiling, 4 mL of 1% trisodium citrate aqueous solution was added immediately under vigorous stirring and reacted for 20 min. Then the mixture was cooled to room temperature. The average diameter of gold particles was about 20 nm according to transmission electron microscopy (TEM) images.

Typically, 1-mL pre-prepared colloidal gold was washed by centrifugation and a red color purified colloidal gold was obtained. Then 4 μL of 1-mmol/L 4MBA (in ethanol) was slowly added to the colloid under vigorous stirring and the resultant mixture was allowed to react over night to immobilize those Raman reporter molecules to gold surface. The reporter-labeled colloids were then separated from solution by centrifugation at 10000 rpm for 30 min. The clear supernatant was discarded, and the packed fuscous gold sediment was resuspended in 1-mL water. After another twice purifications, the sediment was resuspended by BBS under ultrasonic oscillation. Finally, some 4MBA-labeled Au aggregates with proper size induced by reporter molecules were obtained after centrifugal purification.

The reporter-labeled aggregates were immobilized with antibody. Under gently agitation, 10 μL of 2 mg/mL goat anti-human IgG antibody was added to 1 mL of the reporter-labeled Au aggregates and incubated at 4 ℃ for 2 h. After being centrifuged twice, the dark blue Raman reporter-labeled immuno-Au aggregates were blocked by 10-μL BSA (BBS/3%BSA) to shield the bare sites on the surface of Au aggregates. After 1 h at room temperature, the mixture was centrifuged again. Finally, the 4MBA-labeled immuno-Au aggregates after washing was resuspended in 0.5-mL BBS under ultrasonic oscillation.

The immune substrate for SERS-based immunoassay was prepared on the traditional poly-L-lysine coated glass substrate[29]. A drastically washed glass was coated with a film of poly-L-lysine by spin first. Then a uniform layer of antibody was immobilized on this modified substrate. Briefly, 2-μL goat anti-human IgG antibodies (2 mg/mL in BBS) were pipetted onto the substrate and incubated at 4 ℃ in a moist chamber with a relative humidity of 65%–75% for over 12 h. After rinsing three times with TBS solution for 10 min and washing with deionized water drastically to remove the residual IgG, the activity remained surface was blocked with block solution (3% BSA in BBS) for 3 h at room temperature. This antibody-immobilized SERS activity substrate was then thoroughly rinsed with TBS and deionized water respectively. Finally, after dried under argon gas, the IgG-immobilized immune substrate was stored at 4 ℃ before use.

The SERS-based immunoassay was carried out using a standard sandwich protocol, as shown in Fig. 1. 20-μL human IgG solution (100 μg/mL in BBS) was pipetted onto antibody IgG-immobilized point on the substrate and incubated at 37 ℃. After 2 h, the immune substrate coated with antigen was taken out and rinsed with 0.1% tween 20 solution (TBS/0.1% tween 20) for three times, and then was washed three times with TBS. Following, this substrate was covered with the immuno-sensor (4MBA-labeled immuno-Au aggregates) prepared before.

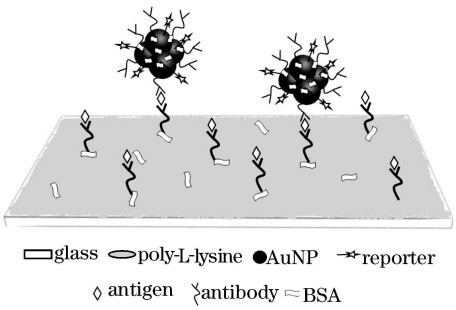

Fig. 1. Sandwich structure of SERS-based immunoassay protocol.

After 2 h at 4 ℃, the substrate was washed with 0.1% tween 20 solution, TBS, deionized water successively and drastically. Finally, this argon gas dried sample was stored at 4 ℃ before SERS detection.

Ultraviolet-visible (UV-Vis) spectrophotometer (UV-3600, Shimadzu, Japan) was applied to monitor the formation of Raman-reporter labeled immuno-Au aggregates. TEM images characterizing the morphology of aggregate were obtained by the TEM (JEM 2000 EX, Jeol, USA) operating at 120-kV accelerating voltage. Field emission scanning electron microscopy (SEM) (Sirion200, FEI, Holand) with 20-kV accelerating voltage was used to characterize the distribution of 4MBA-labeled immuno-Au aggregates after immune recognition. A high speed centrifuge (2-16PK, Sigma, Germany) was used for sample purification. A confocal microscope (FV 1000, Olympus, Japan) assembling a spectrograph (Sharmrock, Andor, UK) with a charge-coupled device (CCD) detector was performed to accomplish SERS measurements. He-Ne laser with 633-nm radiation was used for excitation and the laser power at the sample position was less than 2.3 mW. The scattering light was collected by a 10× objective lens (numerical aperture NA = 0.4) to a CCD detector. The width of the slit was 50 μm and a grating of 1200 lines/mm was used to disperse the scattered light. All SERS spectra reported here were the results of a single 30-s accumulation.

UV-Vis extinction spectra, TEM images, and SERS spectra were recorded to monitor the preparation process of Raman reporter-labeled immuno-Au aggregates and characterize the morphology of gold aggregates, as well as their SERS activity.

The Raman reporter-labeled immuno-Au aggregates were prepared in a two-step process in which the Raman reporter-labeled Au aggregates were fabricated first and then the Raman reporter-labeled immuno-Au aggregates were prepared subsequently. Figure 2 shows the extinction characteristics of gold nanoparticles in different processes. As shown in Fig. 2(a), the citrate capped gold nanoparticles present a strong band with a maximum at 520 nm and some spherical particles with a good monodispersity are displayed in the TEM image shown in the inset of Fig. 2(a).

However, after the addition of 4-μL 4MBA (1.0 mmol/L in ethanol) and centrifugal purification, a significant difference in extinction spectra is observed, as shown in Fig. 2(b). It is clear that the extinction peak of the gold nanoparticles red shifts from 520 to 536 nm. Since the red shift of the surface plasmon resonance

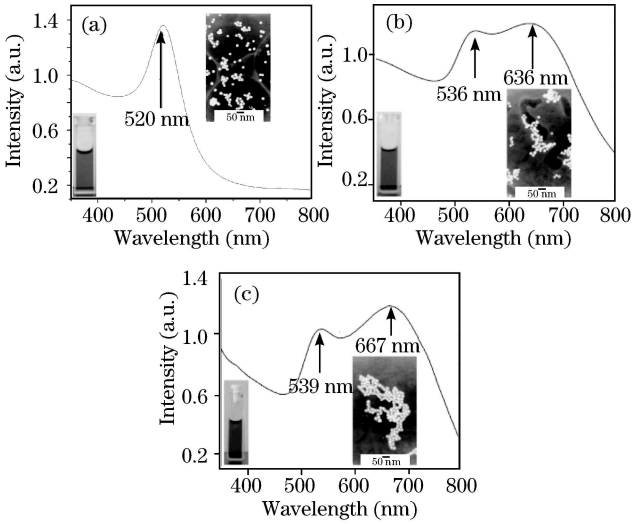

Fig. 2. Characterizations of the Au nanoparticles in different prosesses by UV-Vis extinction spectra and TEM images. (a) Dispersed gold nanoparticles in red with a surface plasma resonance peak at 520 nm show a good monodispersity according to TEM; (b) 4MBA-labeled Au aggregates in navy blue with two surface plasma resonance peaks at 536 and 636 nm are assembled into some chainlike patterns; (c) extinction spectra of dark blue 4MBA-labeled immuno-Au aggregates show a red-shift of both two peaks to 539 and 667 nm, respectively.

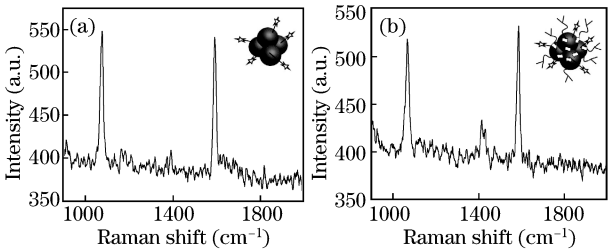

Fig. 3. SERS spectra of (a) 4MBA-labeled Au aggregates and (b) 4MBA-labeled immuno-Au aggregates.

peak corresponds to the increase of particle size[30], it demonstrates the successful binding of 4MBA to the nanoparticles. Moreover, due to the formation of aggregates, the solution color changes from red to navy blue and there is a broad extinction band appearing at the red side of the spectrum with a peak at 636 nm. Mie theory suggests that the plasmon resonance of the aggregates would have an additional long-wavelength component in the extinction spectrum[31]. Repeated experiments have confirmed that the extinction bands of the aggregates induced by 4MBA are reproducible, which indicates that the aggregates with a good repeatability can be obtained controllably. The formation of aggregates was testified by TEM image shown in the inset of Fig. 2(b), and it is clear that with the addition of 4MBA and centrifugal purification, the spherical gold nanoparticles assemble spontaneously into chainlike aggregates. According to our experimental results, it is found that adding 4-μL (1.0 mmol/L in ethanol) 4MBA solution to 1-mL gold colloids can yield the 4MBA-labeled Au aggregates with a good stability and can be stable for several days. Similarly, the SERS activity of those navy blue 4MBA-labeled Au aggregates was tested by SERS scanning in which those novel aggregates acted as not only the SERS signal-generator but also the SERS substrate without any other activation treatment. As displayed in Fig. 3(a), those 4MBA-labeled Au aggregates with a schematic structure shown in the illustration exhibits a strong ability of SERS.

The extinction spectrum of the dark blue 4MBA-labeled immuno-Au aggregates is shown in Fig. 2(c). Two distinctive red-shift peaks of the plasmon resonance at both short and long wavelengths changing from 536 to 539 nm and from 636 to 667 nm are observed respectively, which indicates clearly that the surface residual vacancies of 4MBA-labeled Au aggregates are occupied by antibody IgG[6]. Meanwhile, from the TEM image in Fig. 2(c), it is evident that gold nanoparticles form some longer chainlike assemblies with bigger size. Those IgG-coated 4MBA-labeled Au nanoparticles are well aggregated and can be stable for the next immune protocol. Similarly, according to the two characteristic Raman bands of 4MBA shown in Fig. 3(b), the Raman signals with high signal-to-noise ratio (SNR) are obtained from the immune aggregates, which indicates that this novel type of SERS probe with high SERS activity may have potential use in SERS-based immunoassay.

A highly sensitive SERS-based protein detection using 4MBA-labeled immuno-Au aggregates was identified by comparing with the traditional means using 4MBA-labeled immuno-Au nanoparticles. The result is shown in Fig. 4(a). For the absolutely same assay protocol except for different immuno-sensors, it is obvious that a more sensitive immunoassay can be achieved with the novel sensor proposed by us.

Considering that those 4MBA-labeled immuno-Au aggregates may deposit on the substrate physically without any biologic immune recognition and result in a detection of false positive[8], it is critical to estimate their inimical disturbance for immunoassay. So in the experiment, human antigen IgG (or rat antigen IgG) was chosen as the complementary (or un-complementary) protein for specific (or unspecific) binding with 4MBA-labeled goat anti-human IgG-Au aggregates. The detection results are shown in Fig. 4(b). Clearly, a strong characteristic Raman signal of 4MBA was obtained in the sampling position recognized specifically with human IgG. However,

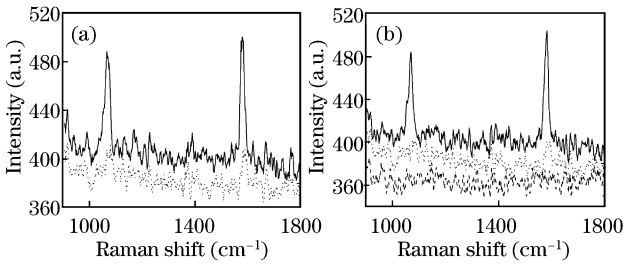

Fig. 4. SERS-based protein detection. (a) More sensitive SERS-based protein detection using 4MBA-labeled immuno-Au aggregates (solid line) in comparison with traditional means with 4MBA-labeled immuno-Au nanoparticles (dotted line). (b) Immunologic specificity detection of 4MBA-labeled immuno-Au aggregates. A strong characteristic SERS signal of 4MBA is obtained in the sampling position recognized specifically with human antigen IgG (solid line) while no similar signal is read out at the point coated with rat antigen IgG (dashed line) or blank regions (dotted line).

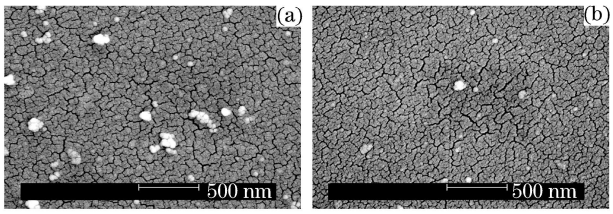

Fig. 5. Patterns of 4MBA-labeled immuno-Au aggregates distribution at different sampling points on the immune substrate. (a) Distribution of aggregates at the point under specific recognition; (b) points without any specific recognition.

because of the non-specificity between the rat IgG and the immune aggregates, after thorough washing, no obviously similar signal was read out at the point coated with rat IgG. Furthermore, some blank regions without any immobilized antibodies but covered with reporter-labeled immuno-Au aggregates were SERS spectra scanned after a series of washing. As shown by the dashed line in Fig. 4(b), after a rigorous washing process, the immuno-Au aggregates absorbed on the immune substrate without any captured human IgG were removed efficiently and the few residue will not pose a tremendous threat to immunoassay. Figure 5 shows the SEM pictures of the distribution of those 4MBA-labeled immuno-Au aggregates after immune recognition. The specific recognition between 4MBA-labeled goat anti-human IgG-Au aggregates and human antigen IgG is revealed obviously in Fig. 5(a), in which some modified aggregates are captured by complementary IgG and some fingerprint spectra of 4MBA with high SNR SERS signal are generated from those aggregates when they are excitated by incidence light. Meanwhile, after some severe washing, few aggregates are absorbed on the immuno-substrate, as shown in Fig. 5(b). All those results correspond with the SERS results obtained above.

According to the above results, it can be deduced that the proposed 4MBA-labeled immuno-Au aggregates have both strong SERS activity and good immune specificity. Such aggregates can be used for a highly sensitive SERS based immunoassay.

In conclusion, a novel SERS immunoassay based on Raman reporter-labeled immuno-Au aggregates is proposed. UV-Vis extinction spectra, TEM images, SEM pictures, and SERS spectra are employed to characterize the products. Experimental results demonstrate that those aggregates with an appropriate size cannot only have high SERS activity but also remain good biological specificity. With those peculiar aggregates, a highly sensitive SERS-based immunoassay is carried out and compared with the traditional Raman reporter-labeled immuno-Au nanoparticles.

This work was supported by the National Natural Science Foundation of China (Nos. 60708024 and 60877024) and the Specialized Research Fund for the Doctoral Program of Higher Education (No. 20070286058).

References

1. P. Pandey, M. Datta, and B. D. Malhotra, Anal. Lett. **41,** 159 (2008).
2. R. L. Garrell, Anal. Chem. **61,** 401A (1989).
3. J. Ni, R. J. Lipert, G. B. Dawson, and M. D. Porter, Anal. Chem. **71,** 4903 (1999).
4. J.-M. Nam, C. S. Thaxton, and C. A. Mirkin, Science **301,** 1884 (2003).
5. C.-C. Lin, Y.-M. Yang, Y.-F. Chen, T.-S. Yang, and H.-C. Chang, Biosens. Bioelectron. **24,** 178 (2008).
6. D. S. Grubisha, R. J. Lipert, H.-Y. Park, J. Driskell, and M. D. Porter, Anal. Chem. **75,** 5936 (2003).
7. Y. Cui, B. Ren, J.-L. Yao, R.-A. Gu, and Z.-Q. Tian, J. Raman Spectrosc. **38,** 896 (2007).
8. J.-W. Chen, Y. Lei, X.-J. Liu, J.-H. Jiang, G.-L. Shen, and R.-Q. Yu, Anal. Bioanal. Chem. **392,** 187 (2008).
9. N. L. Rosi and C. A. Mirkin, Chem. Rev. **105,** 1547 (2005).
10. Z. Zhu, T. Zhu, and Z. Liu, Nanotechnol. **15,** 357 (2004).
11. T. Li, L. Guo, and Z. Wang, Anal. Sci. **24,** 907 (2008).
12. J. T. Krug, II, G. D. Wang, S. R. Emory, and S. Nie, J. Am. Chem. Soc. **121,** 9208 (1999).
13. Y. Jiang, Y. Cui, J.-L. Yao, and R.-A. Gu, Acta Chim. Sin. **64,** 240 (2006).
14. K.-L. Su, H.-H. Huang, T. C. Chang, H.-P. Lin, Y.-C. Lin, and W.-T. Chen, Microfluid Nanofluid **6,** 93 (2009).
15. T. Li, L. Guo, and Z. Wang, Biosens. Bioelectron. **23,** 1125 (2008).
16. M. Yang and C. Wang, Anal. Biochem. **385,** 128 (2009).
17. S. Xu, X. Ji, W. Xu, X. Li, L. Wang, Y. Bai, B. Zhao, and Y. Ozakic, Analyst **129,** 63 (2004).
18. X. X. Han, L. J. Cai, J. Guo, C. X. Wang, W. D. Ruan, W. Y. Han, W. Q. Xu, B. Zhao, and Y. Ozakic, Anal. Chem. **80,** 3020 (2008).
19. M. Manimaran and N. R. Jana, J. Raman Spectrosc. **38,** 1326 (2007).
20. Y. C. Cao, R. Jin, J.-M. Nam, C. S. Thaxton, and C. A. Mirkin, J. Am. Chem. Soc. **125,** 14676 (2003).
21. M. Futamata, Y. Maruyama, and M. Ishikawa, J. Phys. Chem. B **107,** 7607 (2003).
22. C. E. Talley, J. B. Jackson, C. Oubre, N. K. Grady, C. W. Hollars, S. M. Lane, T. R. Huser, P. Nordlander, and N. J. Halas, Nano Lett. **5,** 1569 (2005).
23. F. Svedberg, Z. Li, H. Xu, and M. Kall, Nano Lett. **6,** 2639 (2006).
24. Q. Zhou, G. Zhao, Y. Chao, Y. Li, Y. Wu, and J. Zheng, J. Phys. Chem. C **111,** 1951 (2007).
25. G. H. Gu and J. S. Suh, Langmuir **24,** 8934 (2008).
26. S. Basu, S. Pande, S. Jana, S. Bolisetty, and T. Pal, Langmuir **24,** 5562 (2008).
27. S. Basu, S. K. Ghosh, S. Kundu, S. Panigrahi, S. Praharaj, S. Pande, S. Jana, and T. Pal, J. Colloid Interf. Sci. **313,** 724 (2007).
28. L. O. Brown and S. K. Doorn, Langmuir **24,** 2178 (2008).
29. B. B. Haab, M. J. Dunham, and P. O. Brown, Genome Biol. **2,** research0004 (2001).
30. G. Mie, Ann. Phys. **25,** 377 (1908).
31. P. Galletto, P. F. Brevet, H. H. Girault, R. Antoine, and M. Broyer, J. Phys. Chem. B **103,** 8706 (1999).